

# 3D OBJECT REPRESENTATION WITH TOPO-GEOMETRIC SHAPE MODELS

Sajjad Baloch<sup>†</sup>, Hamid Krim<sup>†</sup>, Irina Kogan<sup>‡</sup>, and Dmitry Zenkov<sup>‡</sup>  
 North Carolina State University, Raleigh, NC 27695

## ABSTRACT

We propose a new method for 3D object representation using weighted skeletal graphs. The geometry of an object is captured by assigning weights to the skeletal graph of the object, which in turn represents its topology. The weights provide necessary information for object reconstruction. The method is rotation, translation, and scaling invariant. Applications include shape representation, compression, and object recognition.

## 1. INTRODUCTION

In this paper, a 3D object to be analyzed is replaced with its 2D boundary, which is assumed to be a compact two-dimensional manifold embedded in  $\mathbb{R}^3$ . It is further assumed that all manifolds of interest are smooth. A short overview of various techniques for 3D shape modeling is given below.

Shinagawa *et al.* [15] proposed an algorithm for modeling the topology of 3D objects using Reeb graphs based on the height function. This approach completely ignores the geometric information of an object. In Osada *et al.* [13], and Hamza and Krim [3], 3D objects are represented through shape distributions, and then a dissimilarity measure for distributions is employed to classify them. Lazarus *et al.* [8] proposed skeletonization based on the geodesic distance from a manually chosen *source point* and called their graphs *level set diagrams*. Hilaga *et al.* [5] extended this approach by eliminating the need for manual selection of a source point and proposing a matching algorithm based on multiresolution Reeb graphs. Although this achieved rotational invariance, the algorithm was computationally intensive. In Kazhdan *et al.* [6] [7], 3D shapes were modeled through a reflective symmetry descriptor defined over a canonical parameterization. Kazhdan and Funkhouser [7] used rotation invariant spherical harmonics as a shape descriptor.

Our approach to capturing the geometry of an object begins with the calculation of a skeletal graph of the object's boundary. We follow [15], [5], [3] in this calculation; however, our choice of a Morse function is different.

<sup>†</sup>Department of Electrical and Computer Engineering.

<sup>‡</sup>Department of Mathematics.

This work was supported by AFOSR F49620-98-1-0190 and NSF CCR-9984067 grants.

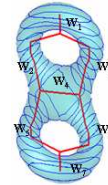


Fig. 1. Weighted skeletal graph: Graph itself captures the topology while graph coupled with the weights  $W_i$  encodes the geometry of the object.

We use the distance function that produces translation, rotation, and scale invariant skeletal graphs. Next, we assign weights to the graph, which is illustrated in Fig. 1. These weights record the information about the shapes of intersections of the object's boundary and the level surfaces of the distance function. Details are given in Section 3. This model is complete in the sense that the original object can be reconstructed, with given precision, from its weighted skeletal graph.

## 2. TOPOLOGICAL MODEL

In this paper, we concentrate on the study of 2D surfaces embedded in  $\mathbb{R}^3$ . The points of  $\mathbb{R}^3$  are represented by their position vectors, which are typed in bold.

### 2.1. Some Definitions

Consider the distance function  $d : \mathbf{p} \mapsto \|\mathbf{p}\|$  in  $\mathbb{R}^3$ . Given a generic surface  $\mathcal{M} \subset \mathbb{R}^3$ , the restriction of the distance function on  $\mathcal{M}$ ,

$$d : \mathcal{M} \rightarrow \mathbb{R}_+, \quad (1)$$

is a Morse function, *i.e.*, all critical points of  $d$  on  $\mathcal{M}$  are non-degenerate (see e.g. [12] and [10]). One can thus use the distance function for constructing a skeletal graph of the surface  $\mathcal{M}$ .

To analyze and encode a compact surface using the Morse function (1), we start at the origin and gradually increase the value of the distance function in  $K$  steps to a sufficiently large number which we denote  $b$ . The integer  $K$  is called the *resolution of the skeletal graph*. Making  $K$  larger increases the precision of captured structural changes in the level sets of the distance function. Recall that such changes occur only at critical level sets.

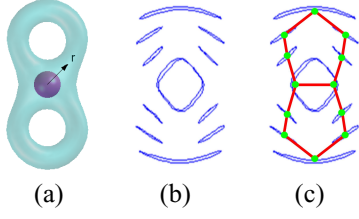


Fig. 2. Skeletal graph of a double torus: (a) Surface analyzed with an evolving sphere; (b) Intersections of the sphere and the surface; (c) Node assignment in the graph.

Since the level sets of  $d$  are concentric spheres, we find intersections of the manifold with spheres of radii  $R$  for all  $R \in [0, b]$  and assign a node to each connected component in an intersection. This is illustrated in Fig.2. The skeletal graph may be described as the quotient space  $\mathcal{M}/\sim$ , where the equivalence relation  $\sim$  is defined below.

*Definition 2.1: (Equivalence)* We say that the points  $\mathbf{p}$  and  $\mathbf{q}$  on the surface are equivalent and write  $\mathbf{p} \sim \mathbf{q}$  if and only if  $\mathbf{p}$  and  $\mathbf{q}$  belong to the same connected component of the level set of the function  $d$ .

Recall the definition of the quotient space:  $\mathcal{M}/\sim := \{[\mathbf{p}] \mid \mathbf{p} \in \mathcal{M}\}$ , where the equivalence class  $[\mathbf{p}]$  of the point  $\mathbf{p} \in \mathcal{M}$  is the set of all points  $\mathbf{q} \in \mathcal{M}$  such that  $\mathbf{q} \sim \mathbf{p}$ .

Note that the function  $d$  given by Eq. (1) is not invariant with respect to translation and scaling. In order to have this invariance, we put the origin at the centroid  $\boldsymbol{\mu}$  of the surface of interest and set

$$d_{\boldsymbol{\mu}}(\mathbf{p}) := \|\mathbf{p} - \boldsymbol{\mu}\|.$$

We then introduce the scaled distance function  $\tilde{d}_{\boldsymbol{\mu}}$  by the formula

$$\tilde{d}_{\boldsymbol{\mu}}(\mathbf{p}) = \frac{d_{\boldsymbol{\mu}}(\mathbf{p}) - d_{\min}}{d_{\max} - d_{\min}}. \quad (2)$$

## 2.2. The Algorithm

The algorithm for computing the skeletal graph is illustrated in Fig. 3 and proceeds as follows:

- Find the centroid of the surface  $\mathcal{M}$  as the arithmetic mean of the vertices of the triangulated mesh and place the origin at the centroid
- Find  $d_{\max}$ , the maximum distance from the centroid to  $\mathcal{M}$
- Given  $K$ , define:

$$r_k := k \frac{d_{\max}}{K}, \quad k = 1, \dots, K$$

- Generate the spheres  $\mathcal{S}_1$  and  $\mathcal{S}_2$  with radii  $R = r_1$  and  $R = r_2$ , respectively
- Find  $\tilde{\mathcal{M}}_p = \mathcal{M} \cap ([\mathcal{S}_1] \cap [\mathcal{S}_2])$ , where  $[\cdot]$  and  $[\cdot]$  identify the interior and exterior of a closed surface;

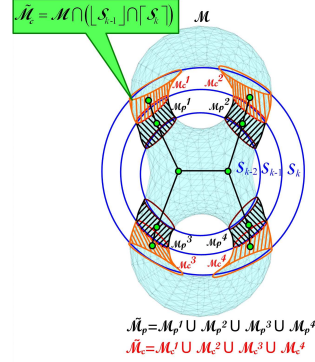


Fig. 3. Skeletonization of a surface  $\mathcal{M}$ .

$\tilde{\mathcal{M}}_p$  is, therefore, the part of  $\mathcal{M}$  that lies between  $\mathcal{S}_1$  and  $\mathcal{S}_2$

- Assign a node  $N_{\mathcal{M}_p}$  to each connected component  $\mathcal{M}_p$  of  $\tilde{\mathcal{M}}_p$  at the centroid of  $\mathcal{M}_p$
- For  $k = 3$  to  $K$ 
  - Generate the “current” sphere  $\mathcal{S}_k$  with radius  $R = r_k$
  - Find  $\tilde{\mathcal{M}}_c = \mathcal{M} \cap ([\mathcal{S}_{k-1}] \cap [\mathcal{S}_k])$ . Hence,  $\tilde{\mathcal{M}}_c$  is the portion of  $\mathcal{M}$  that lies in between  $\mathcal{S}_{k-1}$  and  $\mathcal{S}_k$
  - Find the connected components  $\mathcal{M}_c$  of  $\tilde{\mathcal{M}}_c$
  - For each  $\mathcal{M}_c \in \tilde{\mathcal{M}}_c$  do
    - \* Assign a node  $N_{\mathcal{M}_c}$  at the centroid of  $\mathcal{M}_c$
    - \* Find the connected region  $\mathcal{M}_p \in \tilde{\mathcal{M}}_p$  such that  $\mathcal{M}_c \cup \mathcal{M}_p$  is a single connected region. Add an edge between  $N_{\mathcal{M}_c}$  and  $N_{\mathcal{M}_p}$
  - end for
  - $\tilde{\mathcal{M}}_p = \tilde{\mathcal{M}}_c$
- end for.

## 3. GEOMETRIC REPRESENTATION

In this section we identify the geometry of a 3D object by adding weights to the skeletal graph associated with the distance function. The key idea is to encode the shape of the level curves of the distance function that lie along topologically homogeneous parts of the surface of the object, and to model them subsequently. These level curves are simple closed curves unless they belong to a critical level of the distance function. Once the desired number of the level curves is coded, the remaining ones are restored through a nonlinear interpolation technique known as *elasticae*.

### 3.1. Curve evolution model

Each level set of the distance function is a curve on a sphere. Therefore, after a local coordinate system on a sphere is chosen, the problem of modeling these curves

can be reduced to the problem of modeling planar curves. We typically use the spherical coordinates  $(\theta, \phi)$ , with  $\theta \in [-\pi, \pi]$  and  $\phi \in [-\frac{\pi}{2}, \frac{\pi}{2}]$ . In this setting, we model curves in the rectangle  $\Lambda = [-\pi, \pi] \times [-\frac{\pi}{2}, \frac{\pi}{2}]$ . There is, however, an additional step to perform because the curve evolution model that we are going to adopt here is valid strictly for closed curves. If the original level curve cycles around the  $z$ -axis, its representation in  $\Lambda$  is not a closed curve. There are various ways to address this situation. In some cases, it is enough to rotate the coordinate system in  $\mathbb{R}^3$  in order to move the  $z$ -axis out of the level curve. In other situations, when this rotation may be either impossible or undesirable to perform, we use appropriate coordinates on the sphere to perform our calculations. For instance, when the level curve is close to a big circle on a sphere, the stereographic projection is a good choice of coordinates. In the subsequent discussion, we assume that the curves in  $\Lambda$  are closed.

Let  $\mathcal{C}_r \in \Lambda$  be a closed curve that corresponds to the  $r$ -level curve of the distance function. For such  $\mathcal{C}_r$ , we define the *signed distance field*  $\rho_r : \Lambda \rightarrow \mathbb{R}$  by

$$\rho_r(x, y) = \begin{cases} +D((x, y), \mathcal{C}_r) & \text{if } (x, y) \in [\mathcal{C}_r] \\ -D((x, y), \mathcal{C}_r) & \text{if } (x, y) \in ]\mathcal{C}_r[. \end{cases} \quad (3)$$

In the above,  $D((x, y), \mathcal{C}_r)$  denotes the distance from the point  $(x, y)$  to the set  $\mathcal{C}_r$ , i.e.,

$$D((x, y), \mathcal{C}_r) = \min_{(u, v) \in \mathcal{C}_r} \tilde{D}((x, y), (u, v)),$$

where  $\tilde{D}$  is the Euclidean distance, and  $[\mathcal{C}_r]$  and  $] \mathcal{C}_r [$  represent the interior and exterior of  $\mathcal{C}_r$ , respectively.

The space  $\Omega(\Lambda)$  of closed curves on  $\Lambda$  is infinite-dimensional. In practice,  $\Omega(\Lambda)$  is approximated by a finite-dimensional vector space  $\mathbb{R}^n$ . We write this as  $\rho : \Omega(\Lambda) \rightarrow \mathbb{R}^n$ . Thus, given curves  $\mathcal{C}_1, \dots, \mathcal{C}_m$  at levels  $r_1, \dots, r_m$ , we obtain a collection of  $m$  points,  $\rho_1, \dots, \rho_m$  in  $\mathbb{R}^n$ . Our goal is to model a smooth trajectory that best fits these points. We adopt the elasticæ approach [9]. That is, we fit curve segments between each pair of consecutive points  $\rho_j$  and  $\rho_{j+1}$  and require that

- The overall trajectory minimizes the cost functional

$$E(\alpha) = L \int_0^L \kappa_\alpha^2(s) ds; \quad (4)$$

- the tangent lines to the curve segments  $\rho_{j-1}\rho_j$  and  $\rho_j\rho_{j+1}$  at  $\rho_j$  are the same.

The latter requirement induces the boundary conditions for the cost functional (4). Here and below, curves  $\alpha : [0, L] \rightarrow \mathbb{R}^3$  are parameterized by the arc length and  $\kappa_\alpha(s) = \|\alpha''(s)\|$  is the absolute value curvature of  $\alpha$  at  $s \in [0, L]$ .

For minimization, we use the algorithm given in [11]. The process is illustrated in Fig. 4 where, given  $\alpha_2, \alpha_3$  and  $\alpha_4$ , we have fitted elasticæ between successive pairs

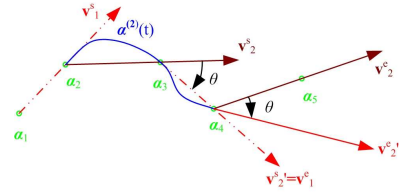


Fig. 4. Two consecutive elasticæ segments with aligned starting and ending tangents.

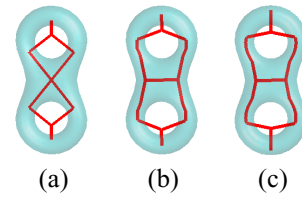


Fig. 5. Skeletal graphs for a double torus: (a)  $K = 4$ ; (b)  $K = 8$ ; (c)  $K = 16$ .

of points  $(\alpha_2, \alpha_3)$  and  $(\alpha_3, \alpha_4)$ . Thus, for any value  $r$  of the distance function  $d$ , we first find the curves  $\alpha(s)$  and  $\rho(s)$  from the elasticæ model and then find the corresponding signed distance field  $\rho_r$ . The zero level set of  $\rho_r$  represents the (reconstructed) level curve of the distance function.

#### 4. TOPO-GEOMETRIC MODEL

As mentioned in the previous section a part of the surface that corresponds to an edge of the skeletal graph is represented by a smooth trajectory. This trajectory is composed of elasticæ segments between successive points in  $\mathbb{R}^3$ . A trajectory, in turn, may be approximated by its spline. Topological and geometrical information is, therefore, combined by weighting each edge of the skeletal graph with the corresponding spline coefficients. Since these weights represent the geometry of the part of the surface along an edge, the weighted skeletal graph is the signature of a given surface. Therefore, the problem of recognition of a 3D object reduces to the matching problem of weighted graphs

#### 5. EXPERIMENTAL RESULTS

Skeletal graphs of three 3D objects are given in Figs. 5–7. In addition, Fig. 7 illustrates the rotational invariance of the proposed technique.

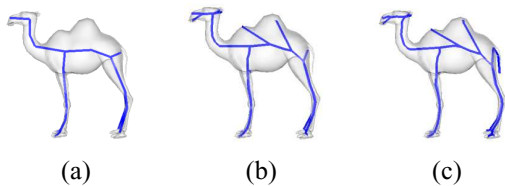


Fig. 6. Skeletal graphs for a camel: (a)  $K = 8$ ; (b)  $K = 16$ ; (c)  $K = 32$ .

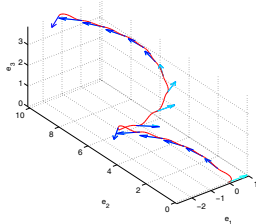


Fig. 9. The critical curve of the elasticæ functional.

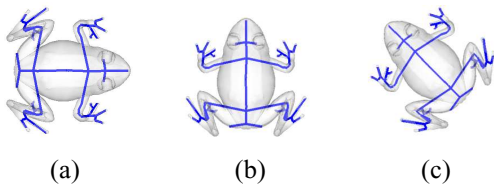


Fig. 7. Rotational invariance of a skeletal graph: (a) No rotation; (b) Rotation by  $\pi/2$ ; (c) Rotation by  $3\pi/4$ .

We give some details on the procedure of capturing the geometry of a double torus. Consider the edge  $\gamma$  of the skeletal graph that corresponds to the highlighted part of the surface in Fig. 8(a). The surface is sampled with  $K = 100$ , which gives 98 level curves along this edge. The optimal tree gives a minimal set of 13 curves, removing redundant curves, a reduction by a factor of 7.54. The elasticæ model is then applied, resulting in the trajectory given in Fig. 9. From the model, we sampled several curves which are rendered in Fig. 8(b). The spline coefficients are eventually assigned to arc  $\gamma$  as weights. The entire reconstructed surface is shown in Fig. 8(d). A more complicated example is given in Fig. 10.

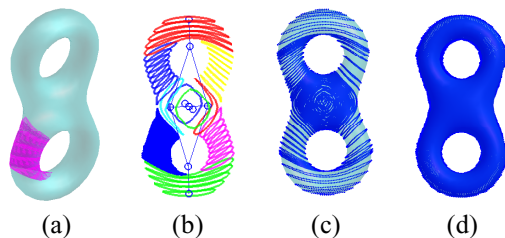


Fig. 8. Surface modeling for a double torus: (a) Level curves of the distance function along the edge  $\gamma$ ; (b) Reconstructed part of the surface along the edge  $\gamma$ ; (c) Optimal curve set; (d) Reconstructed double torus.

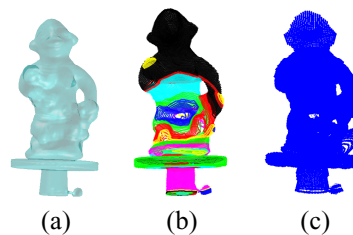


Fig. 10. Reconstruction of the Twins: (a) Original object; (b) Color coded level curves; (c) Reconstructed object.

## 6. CONCLUSIONS

In this paper we proposed a 3D object representation that is rotation, scale and translation invariant. The geometry of an object is captured by assigning weights to the distance-function-based skeletal graph. The resulting weighted graph may be used for object recognition and compression.

## REFERENCES

- [1] S. H. Baloch, H. Krim, W. Mio, and A. Srivastav, "3D Curve Interpolation and Object Reconstruction", *Proc. ICIP'05*, 2005.
- [2] S. H. Baloch, H. Krim, W. Mio, and A. Srivastav, "Topological-geometric shape model for object representation", To be submitted.
- [3] A. B. Hamza, and H. Krim, "Topological modeling of illuminated surfaces using Reeb graphs", *Proc. ICIP'02*, Vol. 1, pp. 769-772, September 2002.
- [4] A. B. Hamza, and H. Krim, "Geodesic object representation and recognition", *Proc. DGCI'03*, pp. 378-387, November 2003.
- [5] M. Hilaga, Y. Shinagawa, T. Kohmura, and T. L. Kunii, "Topology Matching for Fully Automatic Similarity Estimation of 3D Shapes", *Proc. SIGGRAPH'01*, pp. 203-212, August 2001.
- [6] M. Kazhdan, B. Chazelle, D. Dobkin, A. Finkelstein, and T. Funkhouser, "A Reflective Symmetry Descriptor", *European Conference on Computer Vision*, May 2002.
- [7] M. Kazhdan, and T. Funkhouser, "Harmonic 3D Shape Matching", *SIGGRAPH'02 Technical Sketches*, pp. 191, July, 2002.
- [8] F. Lazarus, and A. Verroust, "Level set diagrams of polyheral objects", *Proc. Fifth ACM symposium on Solid Modeling and Applications*, pp. 130-140, June 1999.
- [9] Mumford, D. [1994], *Elastica and Computer Vision*, in *Algebraic Geometry and its Applications (West Lafayette, IN, 1990)*, 491-506, Springer, New York.
- [10] Y. Matsumoto, *An Introduction to Morse Theory*, American Mathematical Society, 1997.
- [11] W. Mio, A. Srivastava, and E. Klassen, Interpolations with elasticæ in Euclidean spaces, *To appear in Quarterly of Applied Mathematics*.
- [12] J. Milnor, *Morse Theory*, Princeton University Press, Princeton, NJ, 1963.
- [13] R. Osada, T. Funkhouser, B. Chazelle, and D. Dobkin, "Shape Distributions", *ACM Transactions on Graphics*, 21(4), pp. 807-832, October 2002.
- [14] G. Reeb, "Sur les points singuliers d'une forme de Pfaff complètement intégrable ou d'une fonction numérique", *Comptes Rendus de L'Académie ses Séances*, Paris, 222, pp. 847-849, 1946.
- [15] Y. Shinagawa, and T. L. Kunii, "Constructing a Reeb graph automatically from cross sections", *IEEE Computer Graphics and Applications*, 11(6), pp. 44-51, November 1991.